Article ID: 1000-7032(2012)08-0808-04

Study on Long-wavelength Optical Phonons in Hexagonal InAlGaN Crystals

CHEN Gui-chu[1,2*], FAN Guang-han[1]

(1. *Institute of Optoelectronic Material and Technolochy, South China Normal University, Guangzhou* 510631, *China*;
2. *Department of Physics, Zhaoqing University, Zhaoqing* 526061, *China*)

* *Corresponding Author, E-mail: gchenbox@163.com*

Abstract: The optical phonons are investigated experimentally by means of Raman scatterning and by the modified random element isodisplacement (MREI) model in hexagonal quaternary nitride-based crystals. A one-mode behavior of E_1 and A_1 branches is presented in our calculated results. The calculated A_1(LO) branches are almost consistent with our experimental data for $In_xGa_{0.45-x}Al_{0.55}N$ crystals, and Cros's experimenatal results for $In_xAl_{0.42-x}Ga_{0.58}N$ crystals.

Key words: InAlGaN; optical phonon; Raman scattering; MREI

CLC number: O433; O484 **Document code**: A **DOI**: 10.3788/fgxb20123308.0808

六方系 InAlGaN 晶体的长波长光学声子研究

陈贵楚[1,2*], 范广涵[1]

(1. 华南师范大学 光电子材料与技术研究所, 广东 广州 510631;
2. 肇庆学院 物理系, 广东 肇庆 526061)

摘要: 利用拉曼散射实验方法对六方系 InAlGaN 晶体的光学声子进行了测量,同时利用修正随机元素同向位移模型对其光学声子与组分的关系进行了理论模拟。结果表明 InAlGaN 晶体的 E_1 与 A_1 光学声子分支都表现为单模行为,测量得到的 $In_xGa_{0.45-x}Al_{0.55}N$ 晶体的 A_1(LO)声子与计算结果一致。对 $In_xAl_{0.42-x}Ga_{0.58}N$ 晶体的 A_1(LO)声子的计算结果与 Cros 的测量结果进行了对比,两者也相符。

关 键 词: InAlGaN; 光学声子; 拉曼散射; MREI

1 Introduction

Ⅲ-nitride alloys have attracted much attention because of their many applications in optoelectronic devices operating from blue-green to ultraviolet range. Great progress has been made in the fabrication of ternary InGaN and AlGaN film[1-2]. Due to In or Al content incorporation into the ternary alloys, the In(Al)GaN/GaN heterostructure induces the large lattice mismatch, which can arise piezoelectric field that influences the emission efficiency[3-6]. In order to solve this problem, several researchers

收稿日期: 2012-04-06; **修订日期**: 2012-06-17
基金项目: 国家自然科学基金(61176043); 肇庆学院自然科学基金(201109)资助项目
作者简介: 陈贵楚(1973-), 男, 湖南岳阳人, 主要从事光电子材料与器件的研究。
E-mail: gchenbox@163.com

utilized lattice and bandgap engineering to grow the quaternary InAlGaN alloy[7-9], whose bandgap and lattice constant can be independently adjusted by varying In and Al compositions, and one can obtain the lattice-matched hexagonal heterostructures with the required band gap. Besides, InAlGaN alloy has the potential for providing a good thermal match to GaN, which could be an advantage in epitaxial growth.

The purpose of this work is to study one of the basic physical properties of Ⅲ-N semiconductors, including the optical phonon, especially the optical-phonon-mode behavior in quaternary semiconductors and InAlGaN alloys crystallize in the wurtzite structure, with space group C_{6v}^4. Among the optical phonons, those having A_1 and E_2 modes are Raman active detected by Raman scattering with back scattering configuration. However, few research is about the optical phonons in InGaAlN alloys, except that Cros made a Raman scattering study[10]. We first use the MREI model treat with the optical phonons of hexagonal quaternary nitride-based crystals, and we also make Raman scattering study for the $A_1(LO)$ phonons of $In_xGa_{0.45-x}Al_{0.55}N$ samples. The calculated results are consistent with our experimental data.

2　Experiments

InAlGaN epilayers were grown by MOCVD in Thomas Swan system on (0001) sapphire substrates. TMIn, TMGa, TMAl, and NH_3 were used as the source precursors for In, Ga, Al, and N, respectively. After pre-baking the sapphire substrates at 1 050 ℃ under hydrogen flow, a 30 nm low-temperature GaN nucleation layer and a 1.2 μm GaN buffer layer were grown at temperatures of 550 ℃ and 1 030 ℃, respectively. 0.6 μm InGaAlN epilayers were grown on the GaN buffer layer at 800 ~ 860 ℃. The composition of InGaAlN alloy was determined by the combination of X-ray double-crystal diffraction and energy dispersive spectroscopy.

The samples were characterized by spatially resolved Raman scattering using 514.5 nm line of an Ar^+ laser. The scattered light was dispersed through the JY-T64000 triple monochromator system attached to a liquid nitrogen cooled CCD detector. The accuracy during the Raman measurements was 0.2 cm with a lateral spatial resolution of 1.0 mm. The samples were excited perpendicular to the substrate surface, and the scattered light was detected in back scattering configuration at 50 mm entrance slit width.

The E_2 and $A_1(LO)$ phonons of three $In_xGa_{0.45-x}Al_{0.55}N$ samples in our experiment, corresponding to three In compositions, *i.e.*, 0%, 5%, 9%, can be detected by Raman scattering. As can be seen in Fig. 1, the off-scale spectra are the strong $A_1(LO)$ phonons at 733 cm^{-1} and E_2 phonons at 563 cm^{-1} for the GaN buffer layer. Weak peaks can be observed at 803, 815, and 823 cm^{-1}, corresponding to $A_1(LO)$ phonons of the quaternary compounds, and they are changed with In composition.

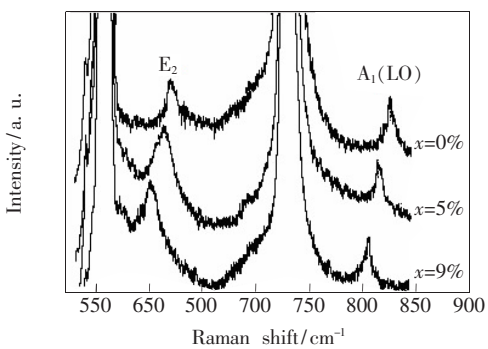

Fig. 1　Optical phonon spectra of $In_xGa_{0.45-x}Al_{0.55}N$/GaN epilayers. The off-scale spectra are the strong $A_1(LO)$ and E_2 phonons of GaN buffer layer. Weak peaks are $A_1(LO)$ and E_2 phonons of InAlGaN crystals, and both are changed with In composition.

3　MREI Model

The MREI model assumes that in the long-wavelength limit of the zone center, the anion and cation of similar species vibrate with the same phase and amplitude, and the forces acting on each atom are given by the statistical average of the interatomic forces between the neighboring atoms, assuming complete randomness. Our samples are grown on a wurtzite structure, unlike the case of cubic crystal, the wurtzite structure is the simplest uniaxial crystal, the governing tensor equations for the optical phonons at the Γ point can be simplified into two

uncoupled equations, *i. e.*, components parallel (E_1 branch) and perpendicular (A_1 branch) to the *c* axis of the crystal.

We have extended the MREI model to the case of wurtzite semiconductor. Considering only nearest-neighbor interactions, the phonon governing equations for wurtzite InAlGaN alloy in the limit are given as follows:

$$m_N\ddot{u}_N = \sum_j x_j f_{jN}(u_j - u_N) + \sum_j x_j e_{jN} E_{loc}, \quad (1)$$

$$m_j\ddot{u}_j = -f_{jN}(u_j - u_N) - e_{jN}E_{loc}, \quad (2)$$

$$p = \sum_j x_j n[e_{jN}(u_N - u_j) + (\alpha_N + \alpha_j)E_{loc}],$$

$$j = \mathrm{In}, \mathrm{Al}, \mathrm{Ga}, \quad (3)$$

$$E_{loc} = (\gamma + C_i)p, \ i = 1, 2, \quad (4)$$

Where, m, u, and e are the atomic masses, the iso-displacement of the atoms from their equilibrium position, and the Szigeti-effective charges of the corresponding binary compounds. f_{jN} is the nearest neighbor bond force. E_{loc} and p are the local electric field and the electric polarization, n is the density of ion pairs, and α is the electronic polarizability. In the equation (3), γ is $4\pi/3$ for the transverse modes, and $-8\pi/3$ for longitudinal modes; meanwhile C_1 is 0.2 for A_1 mode, and C_2 is 0.1 for E_1 mode.

Solving Eq. (3) together with Eq. (4), the local electric field E_{loc} is given by

$$E_{loc} = \frac{1}{\eta}\sum_j x_j e_j (u_j - u_N), \quad (5)$$

where, $\eta = 1/(\gamma + C_i) - \sum_j x_j n(\alpha_j + \alpha_N)$. Making use of the expression of E_{loc} and assuming $U_i (= u_i - u_N)$ varies with time as $\exp(-i\omega t)$, we can mention Eq. (1) and (2) in the form $[\boldsymbol{M}]U = 0$, *with the components of the matrix* $[\boldsymbol{M}]$ gived by

$$M_{ij}(i \neq j) = S_{ij}, \quad (6)$$

$$M_{ii} = \omega^2 + S_{ii} - \frac{f_{iN}}{m_i}, \ i, j = \mathrm{In}, \mathrm{Al}, \mathrm{Ga}, \quad (7)$$

where $S_{ij} = -(1/m_N)x_j f_{jN} + (1/\eta)(e_{iN}/m_i + \sum x_j e_{jN}/m_N)x_j e_{jN}$. The nontrivial solutions for ω can be obtained by setting the determinant of $[\boldsymbol{M}]$ equal to zero. The microscopic parameters involved in Eq. (6) and (7) can be determined from the Born-Huang relations for binary compounds ($x_i = 1$ and $x_{j\neq i} = 0$) (see Eqs. (6) ~ (8) of Ref. [11]). Corresponding to the end members, note that there are two sets of such equations for a ternary compound and three for a quaternary.

4 Results and Discussion

The optical phonon frequencies and high-frequency dielectric constants of binary compounds, used in our calculations, are cited from the Table 1 of Ref. [11]. Fig. 1 exhibits a one-mode behavior for the optical phonon frequencies of E_1 and A_1 branches in $In_xGa_{0.45-x}Al_{0.55}N$ crystals. According to criteria proposed by Chang and Mitra[12], *i. e.*, the atomic mass of nitrogen is much smaller than gallium, indium, and aluminum. The linear composition dependence of LO phonons is presented on the whole In composition. Meanwhile, the TO branches show a rise on the low In composition. The calculated results of A_1(LO) branches are almost consistent with our experimental data.

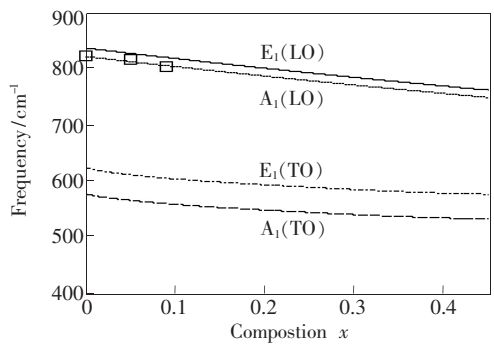

Fig. 2 Optical phonon frequencies of E_1 and A_1 branches for $In_xGa_{0.45-x}Al_{0.55}N$ as a function of In composition x. Squares represent our experimental data of A_1(LO) mode.

Fig. 3 presents the In composition dependency of E_1 and A_1 optical phonons in $In_xAl_{0.42-x}Ga_{0.58}N$. The LO branches exhibit a slight positive bowing on the high In composition, and a rather positive bowing is presented on the whole In composition for the TO branches. The unfilled squares represent the experimental data from Ref. [10], corresponding to four samples with different In compositions, *i. e.*, 0%, 3%, 8%, 10%. The experimental data of the first three samples are consistent with our theoretical results, but the deviation is presented for the fourth sample, as may be the reason that the high In

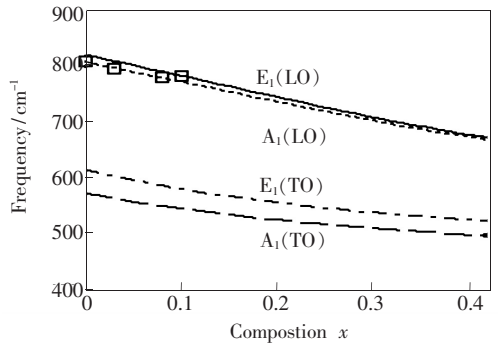

Fig. 3　Optical phonon frequencies of E_1 and A_1 branches for $In_xAl_{0.42-x}Ga_{0.58}N$ as a function of In composition x. Squares represent the experimental data of A_1 (LO) mode from Ref. [10].

composition can cause a little bad effect for the quality of quaternary crystal.

5　Conclusion

We have calculated the optical phonon frequencies of quaternary nitride crystals over the entire compositional range by using MREI model. Both E_1 and A_1 branches exhibit a one-mode behavior in $In_xGa_{0.45-x}Al_{0.55}N$ and $In_xAl_{0.42-x}Ga_{0.58}N$ crystals. The calculated results of A_1(LO) phonons are almost consistent with the experimental data for both crystals.

References:

[1] Akasaki I. Renaissance and progress in crystal growth of nitride semiconductors [J]. *J. Crystal Growth*, 1999, 198(2): 885-893.

[2] Pearton S J, Zolper J C, Shul R J, *et al*. GaN: Processing, defects, and devices [J]. *J. Appl. Phys.*, 1999, 86(1): 1-78.

[3] Chen C Q, Zhang J P, Gaevski M E, *et al*. AlGaN layers grown on GaN using strain-relief interlayers [J]. *Appl. Phys. Lett.*, 2002, 81(26): 4961-4963.

[4] Xing B, Cao W Y, Du W M. Temperature dependent PL of InGaN/GaN multiple quantum wells with variable content of In [J]. *Chin. J. Lumin.* (发光学报), 2010, 31(6): 864-869 (in Chinese).

[5] Xue J S, Hao Y, Zhou X W, *et al*. High quality InAlN/GaN heterostructures grown on sapphire by pulsed metal organic chemical vapor deposition [J]. *J. Crystal Growth*, 2011, 314(1): 359-364.

[6] He T, Chen Y, Li H, *et al*. Optimization of two-step AlN buffer of *a*-plane GaN films grown on *r*-plane sapphire by MOCVD [J]. *Chin. J. Lumin.* (发光学报), 2011, 32(4): 363-367 (in English).

[7] Yu F M, Wang K Q, Shen C W. Influence of polaron effects on the optical absorptions in asymmetrical quantum wells [J]. *Chin. J. Lumin.* (发光学报), 2010, 31(4): 467-472 (in English).

[8] Khan M A, Yang J W, Simin G, *et al*. Lattice and energy band engineering in AlInGaN/GaN heterostructures [J]. *Appl. Phys. Lett.*, 2000, 76(9): 1161-1163.

[9] Herrera M, Cremades A, Piqueras J, *et al*. Study of pinholes and nanotubes in AlInGaN films by cathodoluminescence and atomic force microscopy [J]. *J. Appl. Phys.*, 2004, 95(10): 5306-5311.

[10] Cros A, Cantarero1 A, Pelekanos N T, *et al*. Resonant Raman characterization of InAlGaN/GaN heterostructures [J]. *Phys. Stat. Sol.* (b), 2006, 243(7): 1674-1678.

[11] Yu S G, Kim K W, Bergman L, *et al*. Long-wavelength optical phonons in ternary nitride-based crystals [J]. *Phys. Rev.* B, 1998, 58(23): 15283-15287.

[12] Chang I F, Mitra S S. Application of a modified random-element-isodisplacement model to long-wavelength optic phonons of mixed crystals [J]. *Phys. Rev.*, 1968, 172(3): 924-933.